

An Efficient External Energy Maximization-based Energy Management Strategy for a Battery/Supercapacitor of a Micro Grid System

Mehdi Dhifli^{1*}, Samir Jawadi¹, Abderezak Lashab², Josep M. Guerrero² and Adnane Cherif¹

¹ Research Unite of Processing and Analysis of Electrical and Energetic Systems, Faculty of Sciences of Tunis, University Tunis El-Manar, 2092 Tunis -TUNISIA

² Department of Energy Technology, Aalborg University, 9220 Aalborg East, Denmark.

Abstract

This paper proposes an efficient external energy maximization strategy (EEMS) for a residential micro grid system (MGS). The system sources decomposed into three parts, a photovoltaic (PV) array being a green energy source, an AC grid and a hybrid energy storage system (HESS) (a battery (BT) and supercapacitor (SC)). The proposed strategy aimed at minimizing the grid energy consumption and improve the overall system efficiency by maximizing the BT and SC energy demands within their effective operating limits during the no PV electricity production. This enhance the efficiency of the energy management system during load profile variations. The performance of the proposed EEMS is compared with the PI controller and the equivalent consumption minimization strategy (ECMS) through simulations. A simulation model are developed using Matlab/Simulink to validate all performances.

Key words:

External Energy Maximization Strategy, Renewable Energy, Micro-Grid, Li-ion Battery, Super-Capacitor, Photovoltaic

1. Introduction

Nowadays, solar energy powered micro grid are becoming an alternative potential source for residential applications. Consequently, solar energy powered MGS are becoming an interest energy carrier to replace the traditional fuels. Indeed, PV emerges as one of the most promising candidates for MGS applications[1]-[2]. However, PV is still unable to provide the energy required continuously for the electrical load demand due to its lower power and lower starting density respectively, [3]-[4]-[5].

Nevertheless, the PV drawbacks can be solved by adding a secondary energy sources like batteries or supercapacitors or a both combination [6]. Generally, BTs devices are characterized by their specific higher energy compared to the SCs. Indeed, BTs can provide a long time additional power [7]. However, compared to BTs, SCs are integrated to control transient power due to its high power, higher efficiency and longer charging / discharging cycles[8].

SC is an electrochemical capacitor device that has been chosen to provide an average peak power for short durations [9]. Similar to capacitors, the SC consists of an electrical double layer of non-porous materials (such as pseudo-capacitors) containing transition metal oxides, nitrides and polymers. The electronic power interface is the integration between the power source and the charge which consists of the power converter [10].

The PV was chosen as a potential candidate to convert solar energy into electrical energy. But it can raise concerns such as efficiency, costs and limitations. PV efficiency may depend on system configuration, component design and selection [11].

The cooperation between sources and the required average power optimization are considered the main concerns. For this reason, the Energy Management System (EMS) is included as an interesting solution to control the demand for average required power. However, the main Energy Management System concerns are the operation effectiveness of the control method. Apart from this, the HES Energy Management System faces some challenges in its configuration and application. These latter have been discussed and developed in various studies to provide knowledge and information to the community as a whole. For example, in [12] the paper proposes a new coupled operation of an energy management system with an Adaptive Protection System. In [13] a novel bi-level method is proposed for optimal energy management in hybrid Management of Multi-Micro-grids systems taking into account the Point of Common Coupling line capacity. The proposed method in [14], it is a stochastic energy management algorithm for micro-grids is developed that not only calculates the amount of energy can be delivered to distribution systems, but also considers the reliability of actual loads during emergency states. This paper [15] marks this development and points towards the common functionalities of micro-grid controllers and distributed energy management systems for integration of distributed energy resources into transmission and distribution operations and markets. The authors in [16] propose a complete architecture for a micro-grid management

system based on a multi-agent approach. This article proposes an efficient residential micro grid system configuration, which combines PV, BT and SC. Indeed, the system under study uses PV as the main source to meet the electrical load requirements. A battery and supercapacitor are used as energy backup components that are used to compensate the power deficit. The developed design integrating, PV, BT and SC devoted to residential application is evaluated and investigated using a given real load profile. In addition, throughout this work, the effectiveness and sustainability of a developed energy management system, which is used to improve the system performance, is targeted to optimize the energy generation and to reduce energy consumption. To obtain the required full knowledge characteristics of the system, equivalent consumption minimization strategy control is developed, as will be discussed in details.

The article is organized as follows. Section 2 presents the proposed MGS system configuration. The system modeling presents in section 3. The EMS devoted to the proposed system is developed and detailed in Section 4. The overall efficiency method detailed in section 5. The simulation results are shown in Section 6. Finally, the conclusions are drawn in Section 7.

2. System description and methodology

Fig.1 shows a typical structure of residential power system that consists of the following components:

- Solar PV panels.
- Lithium-ion batteries (BT): They are considered as a long-term power source.
- Super-Capacitor (SC): It is considered as a short-term power source.
- Grid: It is resorted to during low solar irradiance and when the SC and BT are in fully discharged states.
- An efficient external energy maximization strategy (EEMS).
- An apartments and electric vehicles considering that the system is for residential areas.

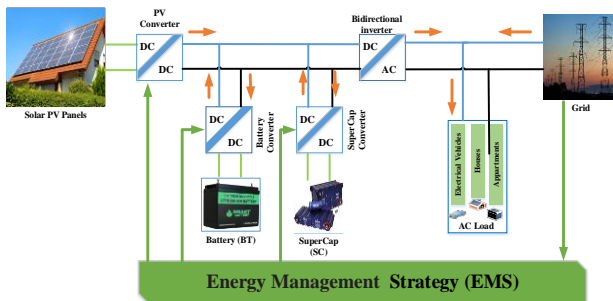


Fig. 1 Overall System Scheme

In this paper, an EEMS for micro-grid system-based residential system is considered (micro-grid for five appartements). The deployment of the latter has become a good option to improve the energy security in all aspects, e.g. reliability, power quality and environmental protections. The PV works as a primary energy source feeding the load and the HESS through a DC-DC converter, which achieves the PV Maximum Power Point Tracking (MPPT) control. An HESS represents a backup source when the power generated by the PV is insufficient to support the AC load. The BT is used, especially, to ensure the power energy coverage during low solar irradiance. Furthermore, the BT can provide the required power during the permanent phases like PV production lack and energy braking. The use of a SC is to supervise and manage the transient and fluctuating power of the energy recovery, due to its fast-dynamic power exchange. A grid is introduced in order to ensure the supply of energy during PV and BT power lacks. An EEMS is proposed to meet the interconnection requirements and to optimize the performance of the power sources and to maintain the sustainability. In order to design an efficient EMS, the system and its dynamics should be well understood; hence, the mathematical model of each component in the system are developed as follows:

3. System Modeling

3.1 PV Model

In order to ensure a maximum efficiency whatever the conditions of sunlight and temperature, the PV strings are connected to a DC-DC converter controlled with an MPPT algorithm. Then, the estimation of the overall electric power PPV produced by the PV surface SPV can be observed as shown in Fig. 2. The PV overall efficiency η_{PV} can be obtained from the next mathematical equations [17] and [18].

$$\begin{cases} P_{pv}(T_a, G_{tot}) = \eta(T_a, G_{tot}) S_{pv} G_{tot} \\ \eta_{pv}(T_c, G_{tot}) = \eta_{manuf} (1 - \beta_{pv} (T_c - T_r)) \\ T_c = T_a + (T_{NOCT} - T_{a,NOCT}) \frac{G_{tot}}{G_{NOCT}} \end{cases} \quad (1)$$

Where T_a is the ambient temperature, G_{tot} is the total solar radiation received by the PV panel, T_c the cell temperature, G_{NOCT} is the nominal solar radiation, T_r is the reference temperature, β_{PV} is the temperature coefficient, and η_{manuf} is the nominal efficiency.

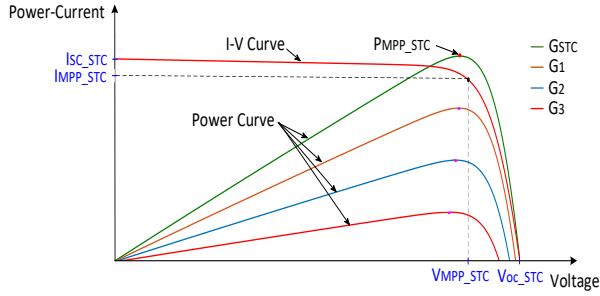


Fig. 2 PV characteristic at different solar irradiance levels (25°C).

3.2 Battery Model

To ensure the simulation stability, a filtered battery current, instead of the actual battery equivalent, is used to account for the polarization resistance [19]. The model parameters are derived from datasheets or simple dynamic tests. From Fig.3, the battery voltage can be expressed as follows [20]-[21]:

$$\begin{cases} I > 0 \rightarrow V = E_0 - K \frac{Q}{Q-it} \cdot it - R_b \cdot I + A_b \exp(-B \cdot it) - K \cdot \frac{Q}{Q-it} i^* \\ I < 0 \rightarrow V = E_0 - K \frac{Q}{Q-it} \cdot it - R_b \cdot I + A_b \exp(-B \cdot it) - K \cdot \frac{Q}{it-0.1Q} i^* \end{cases} \quad (2)$$

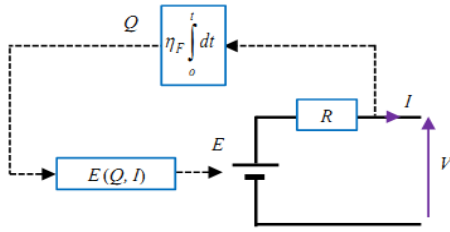


Fig. 3 Battery model

Eq.2 recalls the equations of the Shepherd model for a Li-ion accumulator in case of charge ($I < 0$) and discharge ($I > 0$)

3.3 SuperCapacitor Model

The SCs are included due to their high power density and low equivalent series resistance. These characteristics lead to greater efficiency, higher load current, low heat losses, and longer life span. Therefore, there might be a low risk of fully discharge and can be completely discharged before servicing, which can reduce the electric shock risk during the maintenance period [22]. The SC current-voltage relationship (see Fig. 4) and state of charge are expressed as the following [23]:

$$\begin{cases} U_{SCap} = R_{SCap} \cdot I_{SCap} \cdot \frac{1}{C} \int_0^t (I_{SCap} - I_{SCap}^{DH}) \cdot dt + U_{SCap}(0) \\ SoC_{SCap} = \frac{U_{SCap}^2(t)}{U_{SCap_max}^2(t)} \end{cases} \quad (3)$$

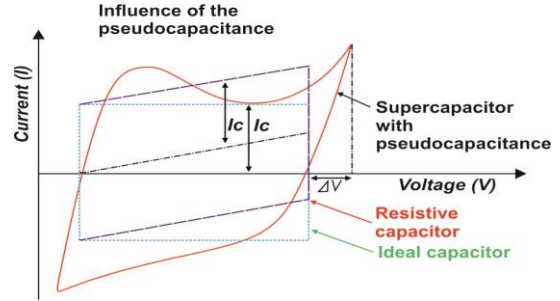


Fig. 4 SC characteristics.

3.4 Load profile

A residential system is adopted in this paper as a micro-grid. Real measurements, which were performed in South Tunisia was used to elaborate a typical day over a month (Fig.5). In the chosen residential area, the heating is non electric and the profile of load depends only on daily activities of consumers (e.g. TV, microwave, refrigerator...) [24]. Variations in the profile of load according to the number of consumers and the seasons were also observed [25].

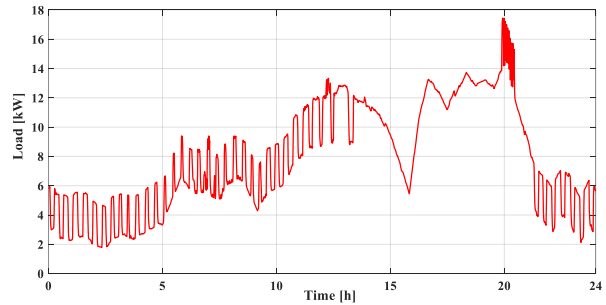


Fig. 5 Load profile

4. Energy Management Strategies

The energy management strategy is developed to ensure a minimized grid energy consumption, a maximized PV production, a long BT and SC life spans, and lower electricity bills with high overall efficiency. To achieve these goals, an EEMS that controls the energy produced by the different energy sources according to the load demand, is developed. In this paper, a control strategy is

proposed based on the aforementioned requirements as shown in Fig. 8. First, the difference between the electric load required by the user (PL) and the generated one from the PV arrays (PPV) is estimated. The difference between these two power terms can represent the power lack or surplus. As expressed in Eq.4, by dividing this difference on the grid and battery and SC operation voltage, it is possible to determine the charging or discharge current (Istorage) which will eventually influence the battery's and SC's SoCs.

$$I_{Storage} = \frac{P_L - P_{PV}}{V_G \text{ or } V_{BT} \text{ or } V_{SCap}} \quad (4)$$

The following sub-sections describe both the classical PI controller-based EMS and the developed ECMS and EEMS in details.

4.1 Classical PI Control Strategy

The energy storage system, which is represented by the battery and SC is controlled by using a PI regulator. The PI regulator reference is calculated by subtracting the load power from the PV power. At each time instant (i), the energy EL used to supply the load and the energy produced by the PV panels EPV are compared. If EPV is greater than EL, the excess energy is used to charge the storage energy system. Otherwise, the storage energy system is discharged to provide the lack of energy. The PI control presented in Fig. 6 takes into consideration the limits SoCmin and SoCmax of the battery. Eq. (5) evaluates the energy difference between the load consumption and the PV production:

$$\Delta E(i) = (P_L[i] - P_{PV}[i])\Delta t \quad (5)$$

Fig. 6 shows an illustration of the PI-based EMS presented in [26] in addition to a slight modification since the energy storage system adopted in this paper consists of two elements.

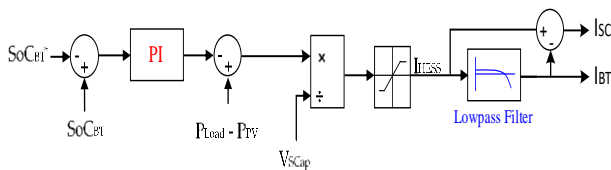


Fig. 6 Energy management scheme: classical PI control.

4.2 The equivalent consumption minimization strategy (ECMS)

The proposed ECMS provides a flexible and highly efficient energy management system, which is controlled

through various parameters, such as the load demand, grid power and BT as well as SC state of charges, respectively (SoCBT/SoCSC). The proposed ECMS aims at minimizing the equivalent grid energy consumption while fixing the battery and super-capacitor state of charge (SoC) within their efficient operating range during all the load profile.

To do this, the control strategy proposed in this work acts to achieve a continuous load supply under various conditions according to a hybrid energy management with an ECMS.

The equivalent energy consumption is proportional to the BT/SC energy times an equivalence factor (β), where β varies with the BT/SC SoC. In this study, the equivalence factor is presented empirically as:

$$\beta = 1 - 2\mu \frac{(SoC - 0.5(SoC_{max} + SoC_{min}))}{SoC_{max} + SoC_{min}} \quad (6)$$

Where SoCmax and SoCmin are maximum and the minimum battery SoCs, respectively. μ is the SoC balance coefficient: $\mu = 0.6$, the value obtained to achieve a minimum SoC of 60% at the end of the mission profile, with an initial SoC of 75%.

As presented in [26], the EMS algorithm is expressed as follows.

Get an optimal solution $x = [P_G, \beta, P_{BT}]$ which minimizes

$$E = [P_G + \beta P_{BT}] \cdot \Delta T \quad (7)$$

Within the equality limitations given by eq (9)

$$P_L + P_G + P_{BT} \quad (8)$$

Under the limiting conditions

$$\begin{aligned} P_{Gmin} &\leq P_G \leq P_{Gmax} \\ P_{BTmin} &\leq P_{BT} \leq P_{BTmax} \\ 0 &\leq \beta \leq 2 \end{aligned} \quad (9)$$

Where E is the equivalent energy consumed by the grid and BT system, respectively, during one sampling time (ΔT).

According to β , it can be observed that, when the BT SoC is below SoCmin, the equivalence factor β is greater than one. Therefore, the equivalent BT energy is more penalized than the grid energy, and the optimization flowchart outputs more grid energy to recharge the BT.

The ECMS is depicted in Fig. 7. The output of the ECMS flowchart is the grid reference power, which is divided by the grid voltage and the dc/dc converter efficiency to get the grid reference current.

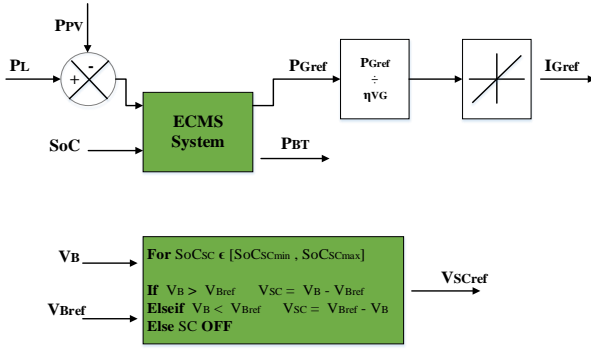


Fig. 7 ECMS

As shown in Fig. 7, the dc bus voltage (or SC voltage) is controlled through a voltage regulator, which outputs the reference currents for the battery converters. The SC equivalent energy is not considered in the optimization problem due to the fact that, in steady state, the load is basically supplied by the fuel cell and the battery systems.

4.3 The external energy maximization strategy (EEMS)

The proposed EEMS aims at minimizing the grid energy consumption by maximizing the BT and SC energy requests within their operating limits. The optimization problem is determined as follows.

Get an optimal solution $x = [P_{BT}, \Delta V]$ which minimizes

$$G = \left[P_{BT} \Delta T + \frac{1}{2} C_r \cdot \Delta V^2 \right] \quad (10)$$

Within the inequality limit

$$P_{BT} \Delta T \leq (SoC - SoC_{min}) V_{BT} Q \quad (11)$$

Under the boundary states

$$\begin{aligned} P_{BTmin} &\leq P_{BT} \leq P_{BTmax} \\ V_{Bmin} - V_B &\leq \Delta V \leq V_{Bmax} - V_B \end{aligned} \quad (12)$$

Where the absolute value $|G|$ is equivalent to the maximum external energy during one sampling time. ΔV is the SC charge/discharge voltage, and C_r is the rated capacitance of the SC. V_{Bmin} and V_{Bmax} are the minimum and maximum dc bus voltage, respectively. V_{BT} and Q are the rated BT voltage and capacity, respectively[27].

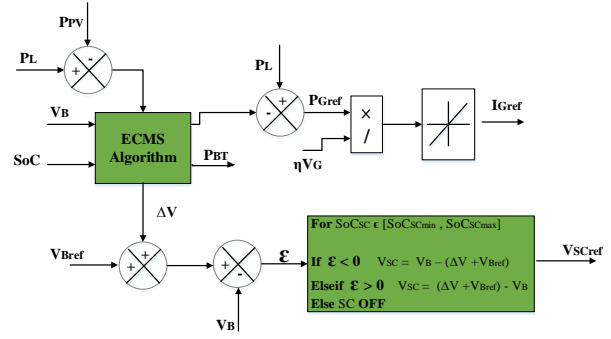


Fig. 8 EEMS

As presented in Fig. 8, the outputs of the EEMS algorithm are the BT reference power and the SC charge/discharge voltage. The BT reference power is afterward eliminated from the load power to get the grid reference power. The SC charge/discharge voltage is added to the dc bus voltage reference to force the SC system to charge or discharge. The dc bus voltage is controlled by the BT converters.

5. Overall system efficiency

The overall system efficiency is evaluated according to the equation (), which is based on the system converters input powers. Therefore, the efficiency (electric efficiency) of the system is defined as the quotient of load power and the sum of all converters input powers. The system electric efficiency is given by

$$\eta_{sys} = \frac{P_L}{P_{PVin} + P_{BTin} + P_{SCin} + P_{Gin}} \quad (13)$$

Where P_{PVin} , P_{BTin} , P_{SCin} and P_{Gin} are the PV power (input to the PV converter), BT power (input to the BT converter), SC power (input to the SC converter) and grid power respectively.

6. Simulation results and evaluations

This part is devoted to the performance evaluation of the proposed EEMS for residential micro-grid system configurations. Indeed, simulation tests were made in Matlab/Simulink environment to obtain the evaluation results, which are then analyzed and discussed in details. The PV, BT, SC and Grid parameters are shown in Table 1.

For performing these tests according to realistic conditions, a real load profile (see Fig. 5). Fig. 9 displays the PV production during the four seasons (In these simulations PV production profile for July) of the year, which were measured in Central-South Tunisia.

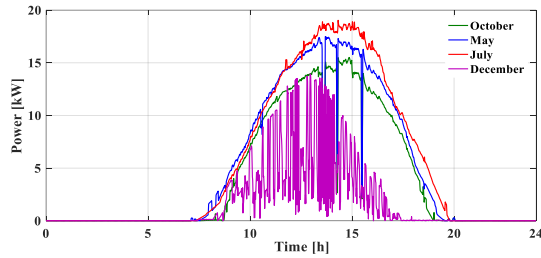


Fig. 9 Average daily production of an 18 kW photovoltaic plant

The rated power of this PV power plant is 18kW. In the proposed PV panel, in order to obtain the results according to the meteorological states, the PV production is multiplied by percentages as follow. 0%: no production. 30%: partial clear sky. 50%: passing cloudiness and 100%: maximum production.

Table 1: This table present the different parameter values of the developed model.

Parameter	Symbol	Value
Photovoltaic Panel (PV)		
Peak power (KW)	$\max(P_{pv})$	18
Surface (m^2)	S_{pv}	40
Nominal efficiency (%)	η_{manuf}	12.35
Reference temperature. ($^{\circ}C$)	T_r	20
Nominal cell temperature. ($^{\circ}C$)	T_{NOCT}	47
Nominal ambient temperature. ($^{\circ}C$)	$T_{a,NOCT}$	20
Nominal solar radiation (W/m^2)	G_{NOCT}	800
Temperature coefficient ($\%/^{\circ}C$)	β_{PV}	0.45
MPPT + converter efficiency (%)	η_{conv}	95
Battery (BT)		
State of charge max (%)	SoC_{BT_Max}	100
State of charge min (%)	SoC_{BT_Min}	20
Battery power (kw)	$[P_{BT_Min} ; P_{BT_Max}]$	[-15 ; 15]
Super-Capacitor (SC)		
State of charge max (%)	SoC_{SC_Max}	90
State of charge min (%)	SoC_{SC_Min}	10
Resistance SC (Ω)	R_{SC}	$6.3e^{-3}$
Capacitance SC (F)	C_0	165

A. System powers and SoCs

Further investigations have been performed by using more EMS strategies. Figures 10, 11 and 12 show the system power variations with EEMS, ECMS and PI strategies, respectively. The simulation results devised on two states, which are:

During Grid connected: In this case, (see Fig. 10) the grid is connected in order to replace the PV and to help the

BT/SC to satisfy all demand power. The BT discharges and supply its maximum power (SoC achieve 26%).

During Grid disconnected: In this case (see Fig. 13), the battery recharges faster to get to its maximum SoC. The PV provides the load power and recharge the BT. The PV power is high, and the SC charge/discharge to help the PV during fluctuations; consequently, the dc bus voltage goes below the reference voltage. Compared to the ECMS (see Fig. 11 and table 2), more BT energy is used (SoC between 26% and 57%).

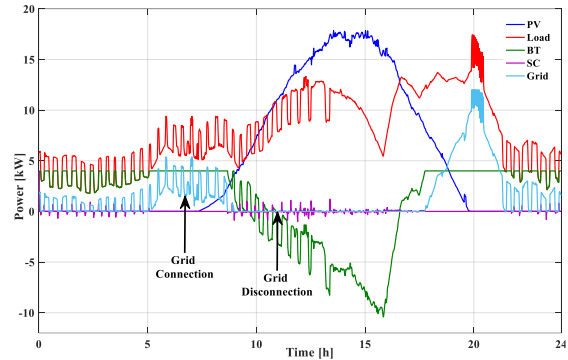


Fig. 10 EEMS power variations

The BT supply more power with EEMS strategy than ECMS in order to decrease the grid energy consumption (see Fig. 10). With the ECMS, the PV continues to recharge the BT well above the minimum SoC (the BT SoC at the end of the mission is 33%), while with the EEMS, the PV power reduces as soon as the minimum BT SoC is reached. Then, this SoC is maintained to 26% throughout the rest of the mission profile.

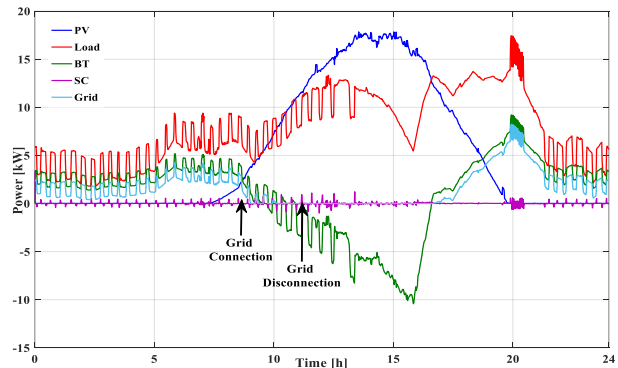


Fig. 11 ECMS power variations

Compared to PI controller (see Fig. 12), the battery works free and supply maximum power (more BT energy is used (SoC between 20% and 50%). With PI controller, the BT and SC supplies maximum power more than the EEMS and ECMS but that affects the efficiency negatively.

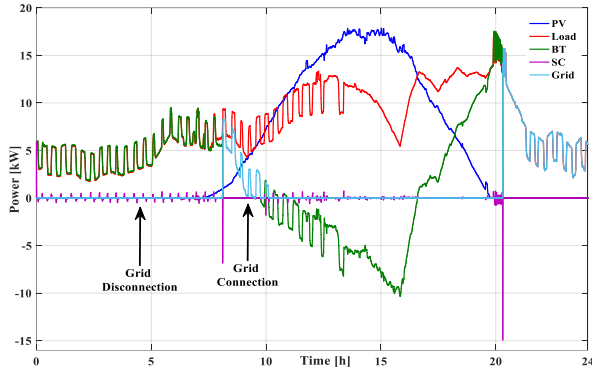


Fig. 12 PI power variations

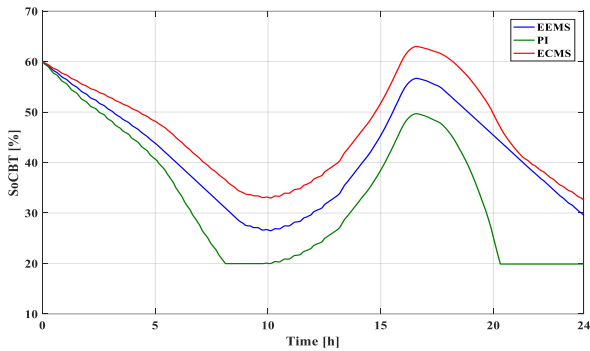


Fig. 13 Battery SoC of EMS strategies

The influence of the fluctuation variations on the load and PV power profiles resolved by using the SC (see Fig. 14).

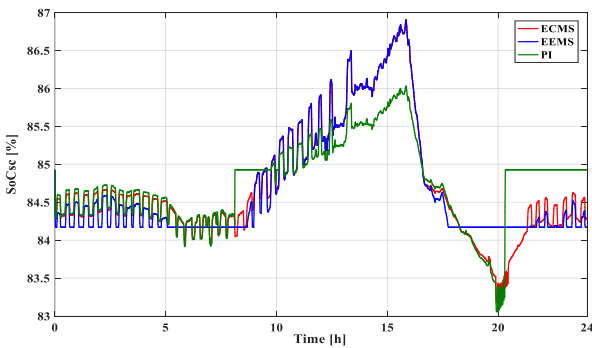


Fig. 14 Supercapacitor SoC of EMS strategies

B. Overall system efficiency evaluation

Fig. 15 and table 2 shows the performances of the EEMS, ECMS and PI. The EEMS is slightly more than ECMS and PI.

The overall system performance varies according to the used EMS strategies. Thus, the best performances have been observed for EEMS (average efficiency achieve

86.5%) compared to the ECMS (average efficiency achieve 85%) and PI (average efficiency achieve 84%) strategies. Therefore, it can be concluded that the EEMS seems to be the most suitable forward strategy since it offers the best features with a constraint of power perturbations compared to the performances of the ECMS and PI strategies.

Table 2: Comparative study with other strategies

	ECMS	PI	EEMS
Average Efficiency (%)	85	84	86.5
Average BT SoC (%)	33-64	20-50	26-57
Average SC SoC (%)	83-86.8	83-86	84.2-86.9

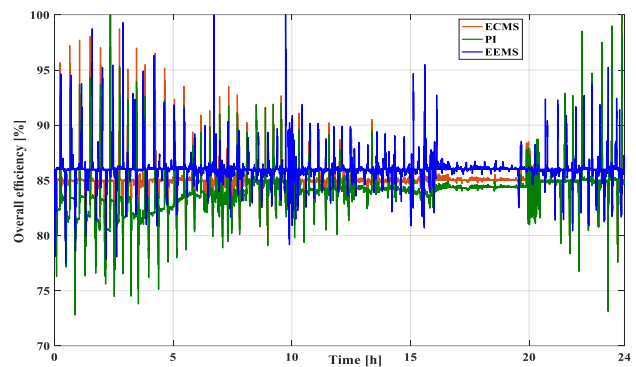


Fig. 15 Overall efficiency comparison of EMS strategies

7. Conclusion

The trend is to the micro grid system (MGS) powered by PV. In this work, we are concerned with a Hybrid Electrical System comprises by PV, BT, SC and Grid. We used PV as a main energy source trends to system supply, the BT / SC as a Backup Energy System and a Grid as a main energy source operate during no PV electricity production. The sustainability challenge of PVs components remains in their stability, efficiency and durability. That is the main reason to include of the BT and the SC as an Energy Backup. Indeed, the backup energy has been integrated to solve the lack power during peak demand periods and to optimize the energy demand. Furthermore, we have applied an accurate EEMS to optimize the power demand through an efficient cooperation between the PV and the proposed energy backup. In so doing the EEMS has been proved and performed through a comparison with other strategies. The proposed strategy, ECMS and PI are compared through simulations. The EEMS was slightly more efficient (15% more efficiency) than the ECMS. A PI controller strategy is also developed to access the performance of the two strategies in terms of efficiency. Finally, the

improvements of MGS system performances are proven through simulation tests.

References

- [1] D. Pavković, M. Lobrović, M. Hrgetić, and A. Komljenović, "A design of cascade control system and adaptive load compensator for battery/ultracapacitor hybrid energy storage-based direct current microgrid," *Energy Convers. Manag.*, vol. 114, pp. 154–167, 2016.
- [2] X. Han, H. Zhang, X. Yu, and L. Wang, "Economic evaluation of grid-connected micro-grid system with photovoltaic and energy storage under different investment and financing models," *Appl. Energy*, vol. 184, pp. 103–118, 2016.
- [3] T. S. Ustun, C. Ozansoy, and A. Zayegh, "Recent developments in microgrids and example cases around the world - A review," *Renew. Sustain. Energy Rev.*, vol. 15, no. 8, pp. 4030–4041, 2011.
- [4] A. M. Vega, F. Santamaria, and E. Rivas, "Modeling for home electric energy management: A review," *Renew. Sustain. Energy Rev.*, vol. 52, pp. 948–959, 2015.
- [5] H. Aouzellag, K. Ghedamsi, and D. Aouzellag, "Energy management and fault tolerant control strategies for fuel cell/ultra-capacitor hybrid electric vehicles to enhance autonomy, efficiency and life time of the fuel cell system," *Int. J. Hydrogen Energy*, vol. 40, no. 22, pp. 7204–7213, 2015.
- [6] C. Yin, H. Wu, F. Locment, and M. Sechilariu, "Energy management of DC microgrid based on photovoltaic combined with diesel generator and supercapacitor," *Energy Convers. Manag.*, vol. 132, pp. 14–27, 2017.
- [7] L. Zacharia et al., "Optimal Energy Management and Scheduling of a Microgrid in Grid-Connected and Islanded Modes," *SEST 2019 - 2nd Int. Conf. Smart Energy Syst. Technol.*, pp. 1–6, 2019.
- [8] D. H. Alamo et al., "An Advanced Forecasting System for the Optimum Energy Management of Island Microgrids," *Energy Procedia*, vol. 159, pp. 111–116, 2019.
- [9] M. M. Morato, P. R. C. Mendes, J. E. Normey-Rico, and C. Bordons, "LPV-MPC fault-tolerant energy management strategy for renewable microgrids," *Int. J. Electr. Power Energy Syst.*, vol. 117, no. October 2019, p. 105644, 2020.
- [10] Y. Xu and X. Shen, "Optimal Control Based Energy Management of Multiple Energy Storage Systems in a Microgrid," *IEEE Access*, vol. 6, pp. 32925–32934, 2018.
- [11] A. Abouarkoub, M. Soliman, Z. Gao, S. Suh, and V. D. Perera, "An Online Smart Microgrid Energy Monitoring and Management System," *2018 6th IEEE Int. Conf. Smart Energy Grid Eng. SEGE 2018*, pp. 58–61, 2018.
- [12] O. Núñez-Mata, R. Palma-Behnke, F. Valencia, A. Urrutia-Molina, P. Mendoza-Araya, and G. Jiménez-Estévez, "Coupling an adaptive protection system with an energy management system for microgrids," *Electr. J.*, vol. 32, no. 10, p. 106675, 2019.
- [13] F. Khavari, A. Badri, and A. Zangeneh, "Energy management in multi-microgrids considering point of common coupling constraint," *Int. J. Electr. Power Energy Syst.*, vol. 115, no. August 2019, p. 105465, 2020.
- [14] J. Najafi, A. Peiravi, A. Anvari-Moghaddam, and J. M. Guerrero, "An efficient interactive framework for improving resilience of power-water distribution systems with multiple privately-owned microgrids," *Int. J. Electr. Power Energy Syst.*, vol. 116, no. September 2019, 2020.
- [15] J. T. Reilly, "From microgrids to aggregators of distributed energy resources. The microgrid controller and distributed energy management systems," *Electr. J.*, vol. 32, no. 5, pp. 30–34, 2019.
- [16] L. Gomes, Z. Vale, and J. M. Corchado, "Microgrid management system based on a multi-agent approach: An office building pilot," *Meas. J. Int. Meas. Confed.*, vol. 154, p. 107427, 2020.
- [17] A. Bouabdallah, J. C. Olivier, S. Bourguet, M. Machmoum, and E. Schaeffer, "Safe sizing methodology applied to a standalone photovoltaic system," *Renew. Energy*, vol. 80, pp. 266–274, 2015.
- [18] A. Bouabdallah, S. Bourguet, J. C. Olivier, and M. Machmoum, "Optimal sizing of a stand-alone photovoltaic system," *Proc. 2013 Int. Conf. Renew. Energy Res. Appl. ICRERA 2013*, no. October, pp. 543–548, 2013.
- [19] B. M. Elektrotechnika, "A dynamic battery model considering the effects of the temperature and capacity fading," pp. 1–10, 2014.
- [20] P. Le Moigne, N. Rizoug, P. Bartholomeüs, K. Chaaban, T. Mesbahi, and F. Khenfri, "Dynamical modeling of Li-ion batteries for electric vehicle applications based on hybrid Particle Swarm–Nelder–Mead (PSO–NM) optimization algorithm," *Electr. Power Syst. Res.*, vol. 131, pp. 195–204, 2015.
- [21] H. Dai, X. Wei, Z. Sun, J. Wang, and W. Gu, "Online cell SOC estimation of Li-ion battery packs using a dual time-scale Kalman filtering for EV applications," *Appl. Energy*, vol. 95, pp. 227–237, 2012.
- [22] L. Shi and M. L. Crow, "Comparison of ultracapacitor electric circuit models," *IEEE Power Energy Soc. 2008 Gen. Meet. Convers. Deliv. Electr. Energy 21st Century, PES*, no. August 2008, 2008.
- [23] W. Li, X. Zhu, and G. Cao, "Modeling and control of a small solar fuel cell hybrid energy system," *J. Zhejiang Univ. A*, vol. 8, no. 5, pp. 734–740, 2007.
- [24] D. Murray, L. Stankovic, and V. Stankovic, "Data Descriptor: An electrical load measurements dataset of United Kingdom households from a two-year longitudinal study," pp. 1–12, 2016.
- [25] A. De Almeida et al., "Residential Monitoring to Decrease Energy Use and Carbon Emissions in Europe."
- [26] S. Njoya Motapon, L. A. Dessaint, and K. Al-Haddad, "A comparative study of energy management schemes for a fuel-cell hybrid emergency power system of more-electric aircraft," *IEEE Trans. Ind. Electron.*, vol. 61, no. 3, pp. 1320–1334, 2014.
- [27] S. N. Motapon, L. A. Dessaint, and K. Al-Haddad, "A robust H₂-consumption-minimization-based energy management strategy for a fuel cell hybrid emergency power system of more electric aircraft," *IEEE Trans. Ind. Electron.*, vol. 61, no. 11, pp. 6148–6156, 2014.